

Electric Potential Around an Absorbing Body in Plasmas: Effect of Ion-Neutral Collisions

S. A. Khrapak, B. A. Klumov, and G. E. Morfill

Max-Planck-Institut für extraterrestrische Physik, D-85741 Garching, Germany

(Received 12 March 2008; published 4 June 2008)

A simple linear kinetic model is used to investigate the combined effect of plasma absorption and ion-neutral collisions on the electric potential around a small absorbing body in weakly ionized plasmas. It is demonstrated that far from the body the potential decays considerably slower than the conventional Debye-Hückel potential. Moreover, at distances exceeding approximately the ion mean free path, the potential approaches an unscreened Coulomb-like asymptote. Some important consequences of this result are discussed in the context of complex (dusty) plasmas.

DOI: [10.1103/PhysRevLett.100.225003](https://doi.org/10.1103/PhysRevLett.100.225003)

PACS numbers: 52.27.Lw

The study of the electric potential distribution around a charged object immersed in an ionized medium is an important basic problem pertinent to a wide variety of physical systems ranging from colloidal suspensions to different aspects of plasma physics, including astrophysical topics, technological plasma applications, probe diagnostics, etc. It is especially important in complex (dusty) plasmas—systems consisting of highly charged micron-size particles in a neutralizing plasma background [1]—since electric interactions are often responsible for the collective behavior of the particle component, e.g., self-organization, formation of ordered (crystal-like) structures, and phase transitions [2,3].

It is usually assumed that the electric potential around a charged spherical grain in isotropic plasmas can be described by the Debye-Hückel (Yukawa) form,

$$\phi(r) = (Q/r) \exp(-r/\lambda), \quad (1)$$

where Q is the grain charge and λ is the plasma screening length. This result can be obtained by assuming Boltzmann distributions for ions and electrons and solving the linearized Poisson equation. Linearization is often invalid in complex plasmas since the grain surface (floating) potential is $\phi_s \sim -T_e/e$ [1] and, therefore, ion-grain coupling is strong close to the grain, provided $T_e \gg T_i$. Nevertheless, numerical solution of the nonlinear Poisson-Boltzmann equation shows that the functional form of Eq. (1) still persists, but the actual value of the grain charge should be replaced by an effective charge which is somewhat smaller in absolute magnitude [4].

A greater influence on the potential is effected by the plasma absorption by the grain. The continuous ion and electron fluxes to the grain surface make their distributions non-Boltzmann. Although the deviations are only marginal for repelled electrons [5], for attracted ions they are quite substantial. In the absence of plasma production and loss in the vicinity of the grain, conservation of plasma flux completely determines the far asymptote of the potential. As a result, at large distances the potential is not screened exponentially but exhibits a power law decay. In collisionless plasmas the far asymptote scales as $\phi(r) \propto r^{-2}$ [1,5]. In the opposite limit of strongly collisional plasma the potential

has a Coulomb-like asymptote, $\phi(r) \propto r^{-1}$ [6,7]. Hence, collisions certainly affect the electric potential around an *absorbing* grain.

There is reason to believe that the collisional contribution to the potential becomes significant even for relatively rare ion-neutral collisions, a typical situation in gas discharges. Recent numerical simulations [8,9], experiments [10,11], and theoretical models [12,13] indicate that the ion flux collected by the grain is affected by collisions even when the ion mean free path ℓ_i is longer than λ . In this weakly collisional regime collisions enhance the ion flux, which leads to a decrease in the absolute magnitude of the grain charge. Since the magnitude of the long-range potential is approximately proportional to the collected flux, the collisional contribution to the potential should be significant even if $\ell_i > \lambda$.

To get further insight into this problem we use a simple linear kinetic model which accounts for the combined effect of ion absorption on the grain and ion-neutral collisions. We consider a small (pointlike) individual grain of negative charge Q immersed in a stationary isotropic weakly ionized plasma. We neglect plasma sources and sinks in the vicinity of the grain, except at the grain surface, which is fully absorbing. This implies that the characteristic ionization or recombination length is considerably larger than the length scale under investigation. For electrons we use a Boltzmann distribution $n_e \approx n_0 \exp(e\phi/T_e)$, where n_0 is the unperturbed plasma density. The kinetic equation for the ions is

$$\frac{\partial f}{\partial t} + \mathbf{v} \frac{\partial f}{\partial \mathbf{r}} + \frac{e\mathbf{E}}{m} \frac{\partial f}{\partial \mathbf{v}} = -\nu(f - n_i f_M) - \delta(\mathbf{r}) \nu \sigma(v) f, \quad (2)$$

where f is the ion velocity distribution function, $f_M = (2\pi v_{T_i}^2)^{-3/2} \exp(-v^2/2v_{T_i}^2)$ is the Maxwellian distribution function normalized to unity, $n_i = \int f d^3v$ is the ion density, and $v_{T_i} = \sqrt{T_i/m}$ is the ion thermal velocity. The first term on the right-hand side is the model collision integral in the Bhatnagar-Gross-Krook form [14] with a *constant* effective ion-neutral collision frequency ν . The second term represents the ion loss on a small grain and is expressed through the effective (velocity dependent) collec-

tion cross section $\sigma(v)$. Such a model kinetic description of ion absorption on a pointlike grain has been recently proposed in Ref. [15] for collisionless plasmas. In this case $\sigma(v)$ can be obtained from the conservation laws of energy and angular momentum, and under some additional assumptions is given by the orbital motion limited (OML) model [1]. In the collisional case $\sigma(v)$ has a less transparent physical meaning and apparently cannot be determined from first principles. However, it is directly related to a “measurable” quantity—the ion flux that the grain collects, $J_i = n_0 \int v \sigma(v) f_M(v) d^3v$. This “normalization” condition will be employed below.

The equations for the electrons and ions are supplemented by the Poisson equation $\Delta\phi = -4\pi e(n_i - n_e) - 4\pi Q\delta(\mathbf{r})$. We linearize these equations assuming $f = n_0 f_M + f_1$, $n_{i(e)} = n_0 + n_{1i(e)}$, $\phi = \phi_1$ and all perturbations are proportional to $\exp(i\mathbf{k}\mathbf{r})$. The result is

$$\begin{aligned} \phi(r) &= \frac{Q}{r} \exp(-k_D r) - \frac{e}{r} \int_0^\infty \frac{k_D \sin(kr) f(\theta) dk}{k^2 + k_D^2} \\ &\equiv \phi_I + \phi_{II}, \end{aligned} \quad (3)$$

where

$$f(\theta) = \frac{8n_0}{\pi^{3/2} k_D} \frac{\int_0^\infty \sigma(\xi) \xi^2 \arctan(\xi/\theta) \exp(-\xi^2) d\xi}{1 - \sqrt{\pi}\theta \exp(\theta^2)[1 - \text{erf}(\theta)]}.$$

Here $k_D = \sqrt{k_{De}^2 + k_{Di}^2}$ is the inverse linearized Debye radius, $k_{Di(e)} = \lambda_{Di(e)}^{-1}$ and $\lambda_{Di(e)} = \sqrt{T_{i(e)}/4\pi e^2 n_0}$, $\theta = (v/\sqrt{2}k v_{Ti}) \equiv (k\ell_i)^{-1}$, and $\xi^2 = v^2/2v_{Ti}^2$. The first term ϕ_I in Eq. (3) is the familiar Debye-Hückel (DH) potential. The second term ϕ_{II} appears due to ion absorption by the grain and accounts for ion-neutral collisions. For a non-absorbing grain [$\sigma(v) \equiv 0$] only the conventional DH form survives, as expected. In this case ion-neutral collisions do not affect the potential distribution.

When the grain absorbs plasma, the term ϕ_{II} is responsible for deviations from the DH form. Let us consider two limiting cases. In the collisionless (CL) limit we have $\nu = 0$, $\theta = 0$, and $\arctan(\xi/\theta) = \pi/2$. The collection cross section is given by the OML model, $\sigma(\xi) = \pi a^2 [1 + (z/\tau)\xi^{-2}]$, where a is the grain radius, $z = |Q|e/aT_e$ is the grain charge in units of (aT_e/e) , and $\tau = T_e/T_i$ is the electron-to-ion temperature ratio. This yields

$$\phi_{II}(r) = -\frac{e}{r} \frac{\pi a^2 n_0 (1 + 2z\tau)}{2k_D} \mathcal{F}(k_D r), \quad (4)$$

where $\mathcal{F}(x) = [e^{-x}\text{Ei}(x) - e^x\text{Ei}(-x)]$ and $\text{Ei}(x)$ is the exponential integral. This expression was recently derived in Ref. [15]. For $x \gg 1$, $\mathcal{F}(x) \approx 2/x$ and the normalized potential is $\frac{e\phi_{II}(x)}{T_e} \approx -\frac{1}{4} \left(\frac{k_D a}{x}\right)^2 \frac{1+2z\tau}{1+z\tau}$, which coincides with the well-known result of probe theory [1,5].

In the opposite strongly collisional (SC) regime we have $\theta \gg 1$, $\arctan(\xi/\theta) \approx \xi/\theta$, and $\text{erf}(\theta) \approx 1 - \pi^{-1/2} e^{-\theta^2} (\theta^{-1} - \frac{1}{2}\theta^{-2})$. The actual form of $\sigma(\xi)$ is not

important since the integral in $f(\theta)$ is directly expressed through the ion flux J_i in this case. We get

$$\phi_{II}(r) \approx -\frac{e}{r} \frac{J_i}{D_i k_D^2} [1 - e^{-k_D r}], \quad (5)$$

where $D_i = v_{Ti}^2/\nu$ is the diffusion coefficient of the ions. This expression coincides with the results obtained using the hydrodynamic approximation [16].

The most interesting regime relevant to the majority of complex plasma experiments in gas discharges is the weakly collisional (WC) regime, $\ell_i \gtrsim \lambda$. In this case we assume $\nu \rightarrow 0$ which yields $\theta \ll 1$, $\arctan(\xi/\theta) \approx \pi/2 - \theta/x$, and $\text{erf}(\theta) \rightarrow 0$. Next, we make an assumption about the functional form of $\sigma(\xi)$. We choose the simplest approximation $\sigma(\xi) = \sigma_0$, which allows us to avoid divergence of the integrals in calculating $f(\theta)$. The value of σ_0 follows from the normalization condition, $\sigma_0 = \sqrt{\pi/8}(J_i/n_0 v_{Ti})$. Integration yields

$$\phi_{II}(r) \approx -\frac{e}{r} \frac{\sqrt{\pi}}{4\sqrt{2}} \frac{J_i}{k_D v_{Ti}} \left\{ \mathcal{F}(k_D r) + \frac{\varepsilon \pi^{3/2}}{\ell_i k_D} [1 - e^{-k_D r}] \right\}, \quad (6)$$

where $\varepsilon = \sqrt{\pi} - 4\pi^{-3/2} \approx 0.60$ is a numerical factor. The two terms in the curly brackets of Eq. (6) correspond to absorption induced “collisionless” and “collisional” contributions, respectively. The collisional contribution to the potential dominates for $r \gtrsim (2/\varepsilon \pi^{3/2}) \ell_i \approx 0.6 \ell_i$. Equation (6) is derived under the assumption $k_D \ell_i \gg 1$, but it yields correct result (to an accuracy of a numerical factor close to unity) also in the opposite limit, $k_D \ell_i \ll 1$, as can be immediately seen by comparing Eqs. (5) and (6). In the CL limit we substitute the OML expression for the ion flux $J_i = \sqrt{8\pi} a^2 n_0 v_{Ti} (1 + z\tau)$ to get $\phi_{II}(r) = -(e/r)(\pi a^2 n_0 / 2k_D)(1 + z\tau) \mathcal{F}(k_D r)$, which is different from the exact expression (4) by a factor $\frac{1+z\tau}{1+2z\tau}$ ($\approx \frac{1}{2}$ since usually $z\tau \gg 1$). This difference is related to our approximation of a *constant* collection cross section while the dominant term in the OML model has a $\sigma(\xi) \propto \xi^{-2}$ scaling.

To proceed further with the quantitative analysis we need to specify the values of J_i and z . Different theoretical models [13,17] for the ion flux as well as formulas that fit the simulation results [9] in a whole range of ion collisionalities are available. However, in addition to the relative complexity of the corresponding expressions, their proper choice requires careful analysis of the approximations involved and applicability conditions. This is beyond the scope of this Letter. Instead, we use two simple approximations providing reasonable accuracy in many practical cases. In the WC regime we employ a simple semiempirical expression $J_i \approx \sqrt{8\pi} a^2 n_0 v_{Ti} [1 + z\tau + 0.1z^2 \tau^2 (k_D \ell_i)^{-1}]$ which provides a reasonable fit for the experimental and numerical simulation data on grain charges in a weakly collisional plasma [1,11] and reduces to the OML expression in the CL limit. In the SC limit the

ion flux collected by a small grain is $J_i \approx 4\pi a n_0 D_i z \tau$ [1,7]. The dimensionless grain charge z is obtained by equating ion and electron fluxes that the grain collect. In the WC regime the electron flux is given by the OML model, $J_e = \sqrt{8\pi} a^2 n_0 v_{T_e} \exp(-z)$. For strongly collisional electrons we have $J_e \approx 4\pi a n_0 D_e z \exp(-z)$ [7]. Then, for fixed gas type, τ , $k_D a$, and $k_D \ell_i$, the normalized electric potential can be calculated.

The results are presented in Fig. 1. The plasma parameters used in these calculations are representative for complex plasma experiments in gas discharges: argon gas, $\tau = 100$, and $k_D a = 0.01$. The solid curves correspond to numerical integration of Eq. (3) for three different ion collisionality indexes $k_D \ell_i$, the dashed curve corresponds to the SC limit, and the dotted curve to the CL limit. For reference, the dash-dotted curve shows the DH potential. Note that the grain surface potentials are different for different curves. This reflects the fact that not only the functional form but also the initial value of the potential at the grain surface depend on the ion collisionality. The inset shows the comparison between direct numerical integration of Eq. (3) and the approximate expression for the WC regime [Eqs. (3) and (6)]. The agreement is rather good and improves with increasing $\ell_i k_D$, as expected.

Figure 1 demonstrates that the long-range asymptote of the potential is dominated by the combined effect of collisions and absorption. It exhibits Coulomb-like decay $\phi(r) \sim Q_{\text{eff}}/r$, where the effective charge Q_{eff} is deter-

mined from the plasma parameters and *increases* in absolute magnitude with ion collisionality. At short distances the potential follows the DH form (1), but the actual grain charge shows a nonmonotonic dependence on $k_D \ell_i$. In the WC regime $|Q|$ decreases with increasing collisionality, while in the SC regime $|Q|$ increases until it reaches a maximum value when electron collection becomes collision dominated [7]. In the WC regime the transition from short-range DH to the long-range Coulomb-like asymptote occurs through an intermediate $\propto r^{-2}$ decay. In the SC regime the potential is Coulomb-like practically from the grain surface. Note the intersection point at $k_D r_* \sim 1$ for the curves corresponding to the WC regime. For $r < r_*$ the absolute amplitude of the potential *decreases* with ion collisionality, while for $r > r_*$ the tendency is opposite.

Let us now briefly discuss some of the consequences of the obtained results.

Intergrain coupling.—Consider the electric interaction between a pair of grains. Assuming for simplicity that the grains have equal charges which are independent of their separation Δ , the interaction energy is $U(\Delta) = Q\phi(\Delta)$. The interesting question is how the intergrain coupling, measured in terms of $U(\Delta)$, varies with the ion collisionality (neutral gas pressure). The answer depends on the ion collisionality rate as well as on intergrain distance. For weak and moderate collisionality $U(\Delta)$ decreases with increasing pressure for $\Delta < r_*$ since both $|\phi(\Delta)|$ and $|Q|$ are suppressed by collisions. For $\Delta > r_*$ the absolute magnitude of the electric potential increases with pressure, but $|Q|$ decreases. Figure 1 indicates that the first effect dominates and, therefore, $U(\Delta)$ increases with pressure. Increasing the pressure further we enter into the SC regime where both $|\phi(\Delta)|$ and $|Q|$ are increasing with ion collisionality. Here the intergrain coupling increases with pressure independently of Δ . This interesting nonmonotonic dependence of coupling on pressure has to be investigated in more detail. Of particular interest would be the possible connection to experimentally observed melting of plasma crystals when reducing gas pressure [3,18].

Phase diagram of complex plasmas.—Complex plasmas are often modeled as an ensemble of grains interacting via DH (Yukawa) repulsive potential. The phase diagram of Yukawa systems has been extensively studied [19] because Yukawa interaction operates in diverse physical systems ranging from elementary particles to colloidal suspensions. The static properties of Yukawa systems are determined by two dimensionless parameters: coupling parameter $\Gamma = Q^2/T\Delta$ and structure (or lattice) parameter $\kappa = \Delta/\lambda$, where T characterizes the kinetic energy of the particle component. Three phases are observed depending on Γ and κ [19]: two solid (bcc at lower κ and fcc at higher κ) at $\Gamma > \Gamma_M$ and a liquid phase at $\Gamma < \Gamma_M$, where Γ_M denotes the coupling parameter at solid-liquid transition. A semi-empirical melting (crystallization) condition $\Gamma_M \approx 106e^\kappa(1 + \kappa + \kappa^2)^{-1}$ yields remarkably good agreement with numerical simulations (for $\kappa \lesssim 10$) and reduces to $\Gamma_M \approx 106$ in the limit of one component plasmas (OCP)

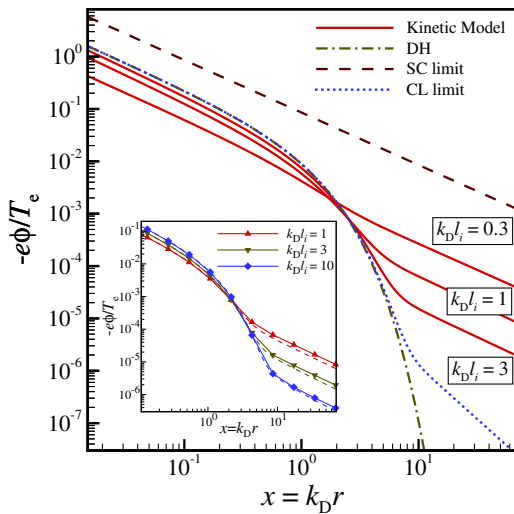


FIG. 1 (color online). Distribution of the normalized electric potential around a small grain in an isotropic weakly ionized plasma for different values of the ion collisionality index $k_D \ell_i$. The solid curves are obtained from Eq. (3). Dashed (dotted) curve corresponds to an analytical approximation in strongly collisional (collisionless) limit. Dash-dotted curve shows the DH potential with the surface potential calculated from (collisionless) OML model. Inset shows the comparison between direct numerical integration of Eq. (3) (solid lines with symbols) and the approximate expression for the weakly collisional regime [Eqs. (3) and (6)] (dashed lines).

[20]. However, it is clear from the results obtained above that ion collisionality should also influence the solid-liquid transition in complex plasmas, at least for $\kappa \geq 1$. For illustrative purposes let us consider the extreme case of strongly collisional plasmas. Combining Eqs. (3) and (5) with the expression for J_i in the SC limit we get $U(r) \approx (Q^2/r)(k_{Di}/k_D)^2[1 + (T_i/T_e)\exp(-k_D r)]$. Since usually $T_e > T_i$, the interaction potential is very close to the Coulomb form for all r . Thus, in this case the phase diagram of Yukawa systems is completely irrelevant. Complex plasmas behave as a Coulomb system of particles with effective charge $Q(k_{Di}/k_D)$ somewhat smaller than the actual charges due to partial plasma screening. The crystallization or melting condition is $\Gamma_M \approx 106(k_D/k_{Di})^2$. For $T_e \gg T_i$ it reduces to $\Gamma_M \approx 106$. For a one-temperature plasma ($T_e = T_i$) we get $\Gamma_M \approx 212$.

Intergrain attraction.—Besides electrical effects, there exist other mechanisms that contribute to intergrain interactions in complex plasmas. These are associated with the (thermodynamic) openness of these systems caused by the continuous exchange of matter and energy between grains and surrounding plasmas. For instance, constant plasma absorption on the grains gives rise to a so-called “ion shadowing” attractive force [21], which represents the ion drag force that one grain experiences in ion flow directed to a neighboring grain. Both long-range electric repulsion and ion shadowing attraction stem from the conservation of the ion flux collected by the grains; both potentials have $\propto r^{-1}$ asymptotes, and depending on their relative magnitudes either attraction or repulsion occurs. Let us derive an approximate condition for attraction. In simplest approximation the ion drag force is proportional to the product of the averaged ion flux density \bar{j}_i , ion momentum \bar{p}_i , and momentum transfer cross section $\bar{\sigma}_{mt}$ for ion-grain collisions. The proportionality coefficient depends on the functional form of $\sigma_{mt}(v)$ as well as on the ion velocity distribution function. For subthermal ion drifts we have $\bar{p}_i = mv_{T_i}$, $\bar{\sigma}_{mt}(v) = \sigma_{mt}(v_{T_i})$, and from flux conservation $\bar{j}_i = J_i/4\pi r^2$. Further, we assume a Maxwellian distribution for the ions and use the modified Coulomb scattering theory [22] to get the momentum transfer cross section, $\sigma_{mt}(v) \approx 4\pi(Qe/mv^2)^2\Lambda$, where Λ is the modified Coulomb logarithm [22]. The resulting ion shadowing potential is $U_{sh} \approx \frac{1}{3}\sqrt{\frac{2}{\pi}}(Qe/r) \times (J_i a/v_{T_i})z\tau\Lambda$. From this we get that $|U_{sh}| > |U_{el}|$ when $k_D \ell_i \geq (3\pi^{5/2}\epsilon/8)(\beta_T\Lambda)^{-1}$, where $\beta_T = |Qe|k_D/T_i$ is the so-called (thermal) scattering parameter [22]. In typical complex plasmas $\beta_T \geq 1$. For a pointlike grain $\Lambda \approx \ln(1 + \beta_T^{-1})$ and thus $\beta_T\Lambda \lesssim 1$. Therefore, the necessary condition for the presence of attraction is $k_D \ell_i \geq (3\pi^{5/2}\epsilon/8) \approx 4$. Note that it is independent of the model used for the ion flux since both potentials are proportional to J_i .

The attraction criterion obtained requires reconsideration of the possibility and conditions for liquid-vapor phase transition and critical point occurrence in complex plas-

mas. These were predicted on the basis of qualitative similarities in interaction as compared to conventional gases (electrical repulsion at short distances and attraction at larger distances due to ion shadowing) [23], however, without considering the effect of ion-neutral collisions.

To summarize, the combined effect of continuous ion absorption and ion-neutral collisions has been demonstrated to determine both the amplitude and the functional form of the electric potential distribution around a small absorbing grain in plasmas. Some important consequences of this result have been briefly discussed in the context of complex plasmas.

This work was supported by DLR under Grant No. 50WP0203.

-
- [1] V. E. Fortov *et al.*, Phys. Rep. **421**, 1 (2005); Phys. Usp. **47**, 447 (2004).
 - [2] J. H. Chu and Lin I, Phys. Rev. Lett. **72**, 4009 (1994); H. Thomas *et al.*, Phys. Rev. Lett. **73**, 652 (1994).
 - [3] H. Thomas and G. Morfill, Nature (London) **379**, 806 (1996).
 - [4] O. Bystrenko and A. Zagorodny, Phys. Lett. A **255**, 325 (1999); A. P. Nefedov, O. F. Petrov, and S. A. Khrapak, Plasma Phys. Rep. **24**, 1037 (1998).
 - [5] Ya. L. Al’pert, A. V. Gurevich, and L. P. Pitaevskii, *Space Physics with Artificial Satellites* (Consultants Bureau, New York, 1965).
 - [6] C. H. Su and S. H. Lam, Phys. Fluids **6**, 1479 (1963).
 - [7] S. A. Khrapak *et al.*, Phys. Plasmas **13**, 052114 (2006).
 - [8] A. V. Zobnin *et al.*, JETP **91**, 483 (2000).
 - [9] I. H. Hutchinson and L. Patacchini, Phys. Plasmas **14**, 013505 (2007).
 - [10] V. E. Fortov *et al.*, Phys. Rev. E **70**, 046415 (2004).
 - [11] S. A. Khrapak *et al.*, Phys. Rev. E **72**, 016406 (2005); S. Ratynskaia *et al.*, Phys. Rev. Lett. **93**, 085001 (2004).
 - [12] M. Lampe *et al.*, Phys. Plasmas **10**, 1500 (2003).
 - [13] L. G. D’yachkov *et al.*, Phys. Plasmas **14**, 042102 (2007).
 - [14] P. L. Bhatnagar, E. P. Gross, and M. Krook, Phys. Rev. **94**, 511 (1954).
 - [15] A. V. Filippov *et al.*, JETP **104**, 147 (2007).
 - [16] S. A. Khrapak *et al.*, J. Appl. Phys. **101**, 033307 (2007); Phys. Rev. Lett. **99**, 055003 (2007).
 - [17] A. A. Lushnikov and M. Kulmala, Phys. Rev. E **70**, 046413 (2004).
 - [18] A. Melzer, A. Homann, and A. Piel, Phys. Rev. E **53**, 2757 (1996).
 - [19] K. Kremer, M. O. Robbins, and G. S. Grest, Phys. Rev. Lett. **57**, 2694 (1986); M. J. Stevens and M. O. Robbins, J. Chem. Phys. **98**, 2319 (1993); S. Hamaguchi, R. T. Farouki, and D. H. E. Dubin, Phys. Rev. E **56**, 4671 (1997).
 - [20] O. Vaulina, S. Khrapak, and G. Morfill, Phys. Rev. E **66**, 016404 (2002).
 - [21] A. M. Ignatov, Plasma Phys. Rep. **22**, 585 (1996); V. N. Tsyтович, Ya. K. Khodataev, and R. Bingham, Comments Plasma Phys. Control. Fusion **17**, 249 (1996).
 - [22] S. A. Khrapak *et al.*, Phys. Rev. E **66**, 046414 (2002).
 - [23] S. A. Khrapak *et al.*, Phys. Rev. Lett. **96**, 015001 (2006).